2010 IEEE International Conference on Robotics and Automation
Anchorage Convention District
May 3-8, 2010, Anchorage, Alaska, USA

Optimization strategies for additional actuators of kinematically redundant parallel kinematic machines

Jens Kotlarski, Trung Do Thanh, Bodo Heimann, and Tobias Ortmaier

Abstract— **In this paper five different optimization strategies for kinematically redundant mechanisms, i.e. mechanisms having additional actuator(s) in at least one kinematic chain, are presented. They are based on two main approaches, a discrete optimization and a classical continuous optimization.**

Exemplarily, a planar, kinematically redundant 3RRR-based mechanism is introduced. The position of its redundant actuator, i.e. the robot geometry, is optimized according to an optimization criterion that is denoted as the gain of the maximal homogenized pose error. Several analysis examples demonstrate the effectiveness of kinematic redundancy with respect to the introduced optimization procedures. It is shown that in comparison to discrete approaches, classical continuous-based optimization strategies do not necessarily lead to more appropriate results in terms of performance improvement.

I. Introduction

In comparison to classical serial mechanisms parallel kinematic machines (PKM) provide a higher accuracy, a higher stiffness, and higher dynamic properties. However, parallel robots suffer from the presence of singularities within their workspace (type-two singularities) [1]. In the vicinity of such configurations actuation forces could tend to infinity. As a result, the kinematic structure can be damaged or even destroyed. Additionally, several performance indices are directly related to the singularity loci [2], e.g. the closer the endeffector (EE) is 'located' to a singularity the higher the pose error is resulting from the influence of active joint errors.

In order to minimize the singularity loci of parallel mechanisms and to increase their performance redundancy can be used [3]. Basically, two redundancy approaches are established for PKM, actuation redundancy and kinematic redundancy [4], [5]. Actuation redundancy can be realized whether by adding a kinematic chain to the mechanism or by actuating a passive joint. Amongst others, it reduces singular configurations and leads to internal preload that can be controlled in order to prevent backlash [6]. However, the control of such mechanisms is a challenging task [7]. Therefore, kinematic redundancy is proposed, obtained by adding at least one actuated joint to one kinematic chain [8], [9]. Thanks to the additional actuator(s), the inverse displacement problem has an infinite number of solutions [10]. Hence, reconfigurations of the mechanism can be performed selectively in order to avoid singularities and to affect its performance directly [11], [12]. It is important to note that with respect to the work of Arakelian et al. [13], kinematic redundancy can be used to rather change the geometrical parameters of a mechanism than its basic structure. This can be done at the task planning stage or while operating the manipulator.

In order to achieve and to maximize the mentioned potentials of kinematic redundancy, an appropriate optimization of the position of the additional actuator(s) is required. Therefore, in this paper, different optimization strategies are presented. They are based on two main approaches: a selective discrete optimization and a classical continuous optimization. These basic approaches can be combined and modified in several ways leading to a single, a discrete, a discrete in case of necessity, a continuous, and a semi-continuous optimization (cp. Section III-A). In each case, the positions/trajectories (depending on the chosen approach) of the redundant actuator(s) are achieved according to a performance index denoted as the gain of the maximal homogenized pose error [14]. It is important to note that the most reasonable way of using the additional actuator(s) highly depends on the application of the mechanism as well as on its properties, e.g. on the resolution and compliance of the redundant actuator(s). The question to be answered in this paper is: does a challenging continuous optimization, i.e. robot control, necessarily outperform simple discrete approaches.

As example, a kinematically redundant version of the well known planar 3RRR mechanism [15] is presented. An additional prismatic actuator is added to an arbitrary base joint. The introduced mechanism is denoted as 3(P)RRR [16]. Several analysis examples demonstrate the efficiency (in terms of an increasing performance) of kinematic redundancy with respect to the introduced optimization procedures. Additionally, the possibility of using 'unnecessary' DOF of the mechanism's EE, i.e. DOF not belonging to the taskspace, to further improve the performance of a PKM is briefly discussed.

The paper is organized as follows. In Section II the geometric model of the exemplarily proposed mechanism is given as well as fundamental definitions related to its Jacobian analysis. Section III clarifies the idea of kinematic redundancy in order to avoid singularities and to increase the performance of a PKM. It gives an overview of different optimization strategies for kinematically redundant mechanisms and introduces the basic optimization procedure. In Section IV several analysis examples are presented in order to demonstrate the effectiveness (in terms of singularity avoidance and, therefore, in terms of accuracy and preci-

All authors are with the Institute of Mechatronic Systems, Leibniz Universität Hannover, Hanover, Germany.
{jens.kotlarski,trung.dothanh,bodo.heimann,
tobias.ortmaier}@imes.uni-hannover.de

sion) of kinematic redundancy with respect to the individual optimization strategies. It is shown that classical continuous optimization strategies are not necessarily able to outperform discrete approaches. Section V concludes this paper.

II. Kinematically redundant 3(P)RRR mechanism

In the following, the geometrical model of the exemplarily analyzed planar, kinematically redundant mechanism is presented. An additional prismatic actuator is proposed allowing one base joint to move linearly. Hence, reconfigurations of the mechanism can be performed selectively while operating the manipulator.

In [16] the kinematically redundant 3(P)RRR planar mechanism (see Fig. 1) is introduced. It is similar to the non-redundant 3RRR mechanism studied amongst others in [15]. Three kinematic chains $G_iM_iP_i$ $(i = 1, 2, 3)$ connect the moving platform $P_1P_2P_3$ to the base $G_1G_2G_3$. Each kinematic chain consists of two links $l_{i,1}$ and $l_{i,2}$. The base-fixed revolute joints are active while the remaining ones are passive. The orientation of the redundant actuator with respect to the x-axis of the inertial coordinate frame $(\mathrm{CF})_0$ is denoted by α. Positions referenced with respect to the platform fixed coordinate frame $(\mathrm{CF})_\mathrm{E}$ are marked with $(')$.

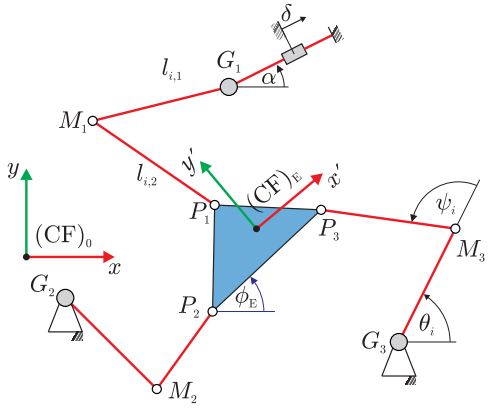

Fig. 1. Kinematically redundant 3(P)RRR mechanism

The configuration of the moving platform is given by

$$\boldsymbol{x} = (x_\mathrm{E},\ y_\mathrm{E},\ \phi_\mathrm{E})^\mathrm{T}, \tag{1}$$

where x_E and y_E represent the point of origin of $(\mathrm{CF})_\mathrm{E}$ with respect to $(\mathrm{CF})_0$ and ϕ_E is its orientation about the z-axis. The mechanism is driven by four actuators. Therefore, the system input is given by the according actuator coordinates

$$\boldsymbol{\theta} = (\theta_1,\ \theta_2,\ \theta_3,\ \delta)^\mathrm{T}. \tag{2}$$

Several performance criteria and indices [17], being possible to optimize the redundant actuator position, can be calculated based on the Jacobian matrices of a PKM, i.e. the Jacobians of the direct $\boldsymbol{A}$ and of the inverse kinematics $\boldsymbol{B}$ (see Section III):

$$\frac{\partial \boldsymbol{f}}{\partial \boldsymbol{x}}\,\dot{\boldsymbol{x}} + \frac{\partial \boldsymbol{f}}{\partial \boldsymbol{\theta}}\,\dot{\boldsymbol{\theta}} = \boldsymbol{0} \ \Leftrightarrow\ \boldsymbol{A}\,\dot{\boldsymbol{x}} + \boldsymbol{B}\,\dot{\boldsymbol{\theta}} = \boldsymbol{0}, \tag{3}$$

where, in this case, $\boldsymbol{f}$ is a 3-dimensional vector including the geometric constraints of each kinematic chain i after elimination of ψ_i for $i = 1, 2, 3$. As long as the Jacobian $\boldsymbol{A}$ is nonsingular, its inverse $\boldsymbol{A}^{-1}$ and, therefore, the overall Jacobian $\boldsymbol{J}$ can be determined analytically:

$$-\boldsymbol{B}\,\dot{\boldsymbol{\theta}} = \boldsymbol{A}\,\dot{\boldsymbol{x}} \quad \Rightarrow \quad \dot{\boldsymbol{x}} = -\boldsymbol{A}^{-1}\,\boldsymbol{B}\,\dot{\boldsymbol{\theta}} = \boldsymbol{J}\,\dot{\boldsymbol{\theta}}. \tag{4}$$

Due to space limitations, the inverse kinematic model as well as a detailed definition of the Jacobians of the mechanism are not presented here. A complete description can be found in [18].

III. Singularity avoidance and accuracy improvement using kinematic redundancy

Thanks to the kinematic redundancy the elements of the Jacobians can be directly affected. As a result, the singularity loci and, therefore, the performance of the mechanism can be modified while operating the system. The effect as well as the use of kinematic redundancy is demonstrated in Fig. 2. The given path would cross a singularity and, therefore, a region suffering from high pose errors for the symmetric, i.e. the 'classical', configuration. By moving the redundant actuator towards the left, the singularity loci change and the manipulator is able to follow the desired path.

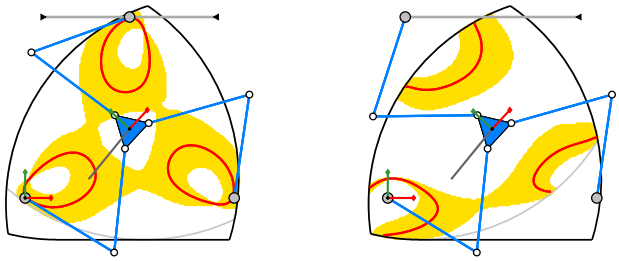

Fig. 2. Trajectory (solid gray) going through a singular configuration (solid red), i.e. through a region where a certain accuracy in one or more DOF is not given (yellow)

A. Optimization strategies of the redundant actuator

In order to exploit the mentioned potentials of kinematic redundancy, an appropriate optimization of the position of the additional actuator is required. This optimization can be performed based on two main strategies: a selective discrete optimization and a classical continuous optimization. These two approaches can be combined and modified in several ways as discussed in the following.

1) Single optimization: The easiest way to use the redundant actuator is to change its position δ only once before starting the desired movement. As a result, the number of reconfigurations is minimized. In case of simple trajectories and repetitive tasks, this approach leads to satisfactory results (in terms of singularity avoidance and performance augmentation). Basically, the idea using a single optimization is to obtain a classical non-redundant mechanism that can be adopted automatically depending on the desired task and, therefore, can be used efficiently for several different applications. The main advantage is that the additional prismatic

actuator remains locked while moving the EE. Hence, energy demand, compliance, e.g. resulting from joint clearance, as well as the control error corresponding to the redundant actuator are minimized. Furthermore, there is no need for any modifications concerning the robot control.

2) Discrete optimization: The discrete optimization is based on the adaption of δ in a discrete manner while operating the system. Therefore, the trajectory is divided into segments. The starting and final points of the segments are certain poses, e.g. shifts in direction ($\dot{\boldsymbol{x}} = \mathbf{0}$). Appropriate constant values of the actuator position δ corresponding to the different segments of the desired trajectory are determined. The resulting set of discrete actuator positions is called the optimized switching pattern. While moving along the desired trajectory, the position of the redundant actuator is changed according to the switching pattern. This allows for the reconfiguration of the mechanism to influence its performance for a given path segment. While performing a reconfiguration the pose of the moving platform is kept constant (in theory). After each switching operation, e.g. while moving along a trajectory segment, the additional prismatic actuator is supposed to remain locked leading to the advantages already mentioned in Section III-A.1.

3) Discrete optimization in case of necessity: In order to minimize the switching operations and to guarantee a certain desired performance the latter mentioned optimization strategy can be additionally modified. The main idea of the discrete optimization in case of necessity is to perform a reconfiguration only if the mechanism is unable to execute the desired operation, e.g. following a singularity-free trajectory and providing a certain performance, in its current configuration [12]. Therefore, before moving the EE, for the upcoming trajectory segment the required performance criteria have to be calculated. If any criteria is less than its corresponding threshold a reconfiguration of the mechanism has to be performed. The optimization procedures and, therefore, the resulting switching operations of the mechanism can be affected directly by an appropriate choice of the required thresholds.

4) Continuous optimization: This optimization strategy leads to a continuously influenceable performance. In contrast to a discrete optimization, the position of the redundant actuator is changed while moving the EE along the desired path. Hence, there is no need to keep the pose of the moving platform constant while performing a reconfiguration, i.e. no additional time is needed to execute the desired task. However, it results in a more challenging robot control and usually in a higher energy demand. Furthermore, the movement of δ is bounded depending on its dynamics and on the system's work cycle time.

5) Semi-continuous optimization: Due to its limited dynamics there might be the case, if using the continuous optimization, that the redundant actuator cannot be moved towards an appropriate configuration sufficiently fast. To overcome this problem, the two strategies mentioned in Section III-A.2 and III-A.4 can be combined. While moving the EE, the position δ is changed continuously (cp. Section III-A.4). At certain poses, e.g. at shifts in direction, an additional discrete optimization is performed while keeping the position and orientation of the EE constant (cp. Section III-A.2).

6) Further Modifications: In some cases there might be the possibility to use certain DOF of the EE to further improve the performance of a mechanism. Regarding a milling process using a PKM, e.g. a Stewart-based mechanism. The orientation around the drill axis can be treated as a redundant degree of freedom. In such cases the additional, i.e. not required, DOF of the EE can be used to further improve the performance of a PKM. Similar to Section III-A.1 - III-A.5 an optimization of the corresponding DOF can be performed and, therefore, combined with the redundant actuator(s) in several ways.

It is important to note that the most reasonable way of using the additional actuator(s) (and DOF of the EE) highly depends on the desired application of the mechanism and on the mechanism itself, e.g. on the resolution and compliance of its redundant actuator(s).

B. Optimization procedure

The optimization can be implemented with respect to several criteria and performance indices [17]. A popular criterion is the condition number of the Jacobian $\boldsymbol{J}$, e.g. the two-norm condition number. However, this does not necessarily exhibit a complete consistent behavior with respect to the performance of a robot (doubtful physical meaning) [17]. Furthermore, it cannot be calculated analytically, i.e. time efficient.

The choice of an appropriate criterion should always depend on the property of the mechanism to be optimized. In this paper the authors focus on two properties, singularity avoidance and improvement of the achievable accuracy. These two properties are directly related. The closer the EE is 'located' to a singular configuration, i.e. to a most relevant type-two singularity [1], the higher is the resulting EE pose error, e.g. due to a limited encoder resolution. Hence, by maximizing the achievable accuracy, i.e. minimizing the pose error, using an appropriate criterion the mechanism's performance can be increased and singularities are avoided at the same time. An approximation of the achievable accuracy, i.e. the pose error $\Delta\boldsymbol{x} = (\Delta x_{\mathrm{E}},\ \Delta y_{\mathrm{E}},\ \Delta\phi_{\mathrm{E}})^{\mathrm{T}}$ and the maximal pose error $\overline{\Delta\boldsymbol{x}}$, respectively, can be determined by rewriting the velocity equation (3) in incremental form [19]:

$$\overline{\Delta\boldsymbol{x}} = |\boldsymbol{J}|\,\Delta\boldsymbol{\theta} \geq |\Delta\boldsymbol{x}|, \tag{5}$$

where $|\boldsymbol{J}| := (|j_{i,k}|)\ \ \forall i,k$ is the modified mechanism's Jacobian and $\Delta\boldsymbol{\theta} = (\Delta\theta_1,\ \Delta\theta_2,\ \Delta\theta_3,\ \Delta\delta)^{\mathrm{T}}$ is the active joint error vector. In general, its elements, i.e. the limited actuator resolutions, are well known from the data sheets.

Regarding the properties to be improved, an optimization of the actuator position δ based on minimizing the two-norm of the maximal homogenized pose error $\overline{\Delta\boldsymbol{x}_{\mathrm{h}}}$ is proposed [14]:

$$\gamma(\overline{\Delta\boldsymbol{x}_{\mathrm{h}}}) = \left|\left|\overline{\Delta\boldsymbol{x}_{\mathrm{h}}}\right|\right|_2 = ||(|\boldsymbol{J}_{\mathrm{h}}|\,\Delta\boldsymbol{\theta})||_2\,. \tag{6}$$

This index is called the gain $\gamma(\overline{\Delta \boldsymbol{x}_\mathrm{h}})$. It is important to note that the Jacobian matrix $\boldsymbol{J}$ is not homogeneous in terms of physical units. Therefore, a homogenization is performed by transforming the moving platform velocity $\dot{\boldsymbol{x}}$ into the linear velocity of two appropriately chosen points, e.g. P_1 and P_2 (see Fig. 1) [20], [14]. This leads to the homogenized Jacobian $\boldsymbol{J}_\mathrm{h}$:

$$\boldsymbol{J}_\mathrm{h} = \begin{pmatrix} \cos\beta & \sin\beta & 0 \\ -\sin\beta & \cos\beta & 0 \\ -\sin\beta & \cos\beta & \|P_2 - P_1\|_2 \end{pmatrix} \boldsymbol{J}, \tag{7}$$

where the angle β gives the orientation of $(\mathrm{CF})_0$ to a coordinate frame $(\mathrm{CF})_{\mathrm{E,h}}$ which is located at P_1 and attached to the moving platform such that its x-axis passes through P_2. Finally, the cost function to be minimized results to:

$$\delta_\mathrm{opt} = \arg\left(\min_{\delta} \gamma(\overline{\Delta \boldsymbol{x}_\mathrm{h}})\right). \tag{8}$$

Depending on the optimization strategy, δ_opt can either be a vector or a single scalar.

The optimization method is based on the golden section search and a parabolic interpolation [21]. The algorithm finds the minimum of a defined cost function within a bounded interval. It does not guarantee to find the global solution of the optimization problem. However, performed tests showed the robustness and efficiency of this approach.

IV. Numerical Results

For different trajectories the effect of the additional prismatic actuator in terms of singularity avoidance and accuracy improvement is demonstrated. It is shown that the achievable performance of the mechanism highly depends on the chosen optimization strategy.

A. Simulation conditions

The geometrical parameters of the exemplarily analyzed kinematically redundant mechanism and its non-redundant counterpart are given in Table I. In the redundant case, one

TABLE I
DESIGN PARAMETERS OF THE ANALYZED 3(P)RRR MECHANISM
$(-0.5\,\mathrm{m} \leq \delta \leq 0.5\,\mathrm{m})$

	$i=1$	$i=2$	$i=3$
x_{G_i} [m]	0.6	0	1.2
y_{G_i} [m]	$\sqrt{27}/5$	0	0
x'_{P_i} [m]	0	-0.1	0.1
y'_{P_i} [m]	$\sqrt{0.12}/3$	$-\sqrt{0.03}/3$	$-\sqrt{0.03}/3$
$l_{i,1}$ [m]	0.6	0.6	0.6
$l_{i,2}$ [m]	0.6	0.6	0.6

prismatic actuator is attached to G_1 of the basic structure. Keeping the design space in mind the orientation of the redundant actuator was set to $\alpha = 0°$. It is important to note that the parameters of the additional prismatic actuator, i.e. its stroke as well as its orientation, were chosen intuitively. Future work will deal with an optimization of the parameters of redundant actuator(s). The active joint errors were set based on data sheets of commercially available standard actuators to $\Delta\boldsymbol{\theta} = (0.025°,\ 0.025°,\ 0.025°,\ 40\,\mu\mathrm{m})^\mathrm{T}$. In the non-redundant case the last element of $\Delta\boldsymbol{\theta}$ vanishes. The maximal force and velocity of the prismatic actuator were set to $F_{\delta,\max} = 500\,\mathrm{N}$ and $v_{\delta,\max} = 3\,\frac{\mathrm{m}}{\mathrm{s}}$. Considering the mass the additional actuator has to move (in case of the experimental test bed existing at the Institute of Mechatronic Systems) the maximal acceleration results to $a_{\delta,\max} = 15\,\frac{\mathrm{m}}{\mathrm{s}^2}$. These values were taken from data sheets as well.

Exemplarily, simulations along the three triangular trajectories (t_I, t_II, t_III) shown in Fig. 3 were performed. The trajectories were chosen within the workspace of the mechanism in order to clarify the effectiveness of the proposed concept as well as the differences of the individual optimization strategies. The EE was moved clockwise along the depicted trajectories with a constant orientation. The overall trajectory time was set to $t_\mathrm{tr} = 1.5\,\mathrm{s}$ (not including any extra time necessary to reconfigure the redundant mechanism). Without loss of generality, the considered 3(P)RRR mechanism is in the following assumed to remain in the same working mode shown in Fig. 1.

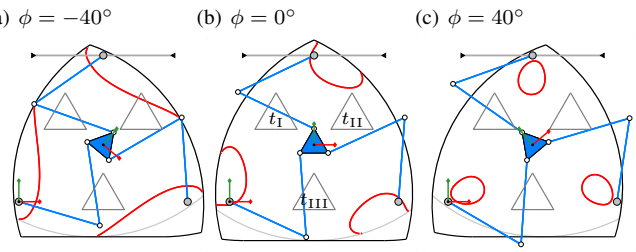

Fig. 3. Exemplarily chosen trajectories t_I, t_II, t_III (solid gray) for the 3RRR-based mechanisms, the solid red lines represent the singularity loci within the workspace (solid black)

In the following, a comparative study on the achievable performance with respect to the optimization procedure is given. In each case, the optimization was performed based on the introduced cost function (8).

B. Optimization strategies - comparison

For the discrete and semi-continuous optimization approaches (Section III-A.2, III-A.3, and III-A.5), the trajectories were divided such that each side of a triangular represents a segment. Hence, at every corner the position of the redundant actuator δ is switched according to the optimized switching pattern. Regarding approach 3, a reconfiguration is only performed if any of the thresholds $\lambda_{1,\min} = 0.01$ corresponding to the absolute value of the Jacobian determinant $|\det(\boldsymbol{A})|$ and $\lambda_{2,\max} = 0.75$ corresponding to the two-norm of the maximal homogenized pose error $\gamma(\overline{\Delta \boldsymbol{x}_\mathrm{h}})$ fall below and are exceeded, respectively. During the discrete switching operations the moving platform pose is supposed to be constant. In case of the continuous optimization, the movement of δ is bounded with respect to the prismatic actuator dynamics given in Section IV-A.

Fig. 4 exemplarily shows the results obtained when moving the EE along trajectory t_I with a constant orientation $\phi_\mathrm{E} = 0°$. The gray marked areas represent the time when the mechanism performs a reconfiguration while keeping the

EE pose constant (in theory). In the non-redundant case these extra trajectory times vanish (for simplification reasons concerning the illustration, the EE pose of the 3RRR mechanism is kept constant in such areas). A significant increase of

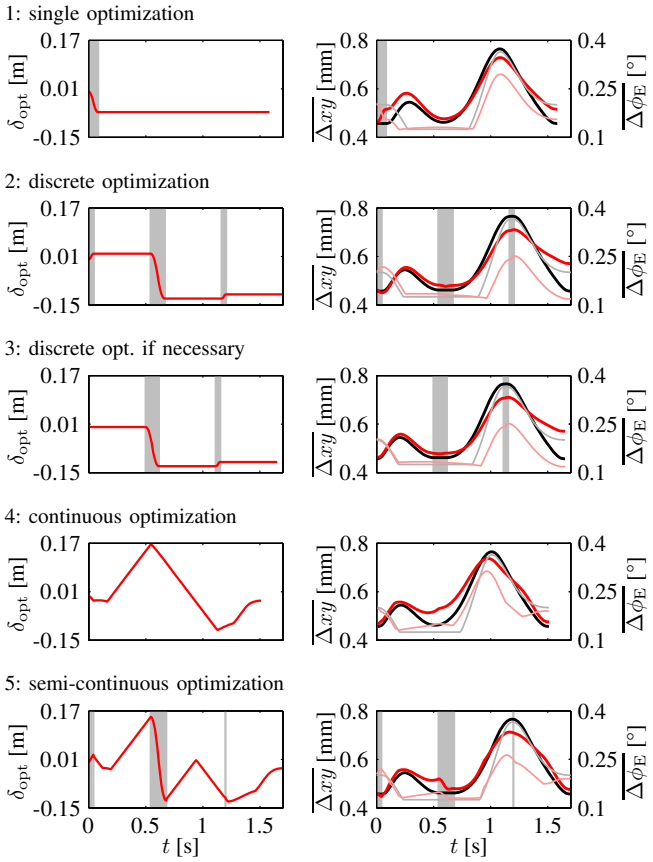

Fig. 4. Simulation results while moving along t_{I} with a constant $\phi_{\mathrm{E}} = 0°$; left: optimized actuator position δ_{opt}, right: maximal positioning error $\overline{\Delta xy}$ (thick black: 3RRR, thick red: 3(P)RRR) and orientational error $\overline{\Delta\phi_{\mathrm{E}}}$ (thin gray: 3RRR, thin light red: 3(P)RRR); gray marked areas indicate a discrete reconfiguration

the pose accuracy due to the kinematic redundancy is well noticeable. The maximum pose error ($t \approx 1.2\,\mathrm{s}$) occurring close to the lower left corner of the triangular trajectory t_{I} (cp. Fig. 3) is more or less minimized by a reconfiguration according to δ_{opt}. It can be seen that the number of switching operations as well as the values of δ_{opt} and, therefore, the trajectory time highly depend on the optimization approach. Furthermore, it is demonstrated that an additional continuous movement of the actuator position δ does not necessarily lead to further improvements concerning the achievable accuracy. This is due to two facts. Firstly, the limited dynamics of the prismatic actuator not allowing for an optimal actuator position without decreasing the EE dynamics. Secondly, in most cases, i.e. for common trajectories going through certain parts of the workspace, a single optimization is sufficient to move the part of the workspace providing a high performance such that the desired trajectory lies within this appropriate area (cp. Fig. 2). Additionally, the latter indicates what the authors noticed while performing several simulations: unrealistic high dynamics, e.g. unlimited dynamics, of the additional prismatic actuator do not significantly further improve the moving platform's maximal pose error over a trajectory. Therefore, the advantage of an implementation of the inconvenient continuous optimization is questionable.

In Table II an overview of the maximal errors of the three triangular trajectories shown in Fig. 3 are given with respect to the optimization strategies 1, 2, 3, 4, and 5 (see Section III-A). In order to quantify the accuracy improvement the maximal translational $\overline{\Delta xy}_{\mathrm{m}}$ and rotational error $\overline{\Delta\phi_{\mathrm{E}}}_{\mathrm{m}}$ of the moving platform over a complete trajectory was determined. Due to its lack of relevance, the initial reconfiguration was not taken into account (it can be performed before starting the desired task). The values represent the achievable accuracy of the associated mechanism. The percentage increase/decrease η of the kinematically redundant PKM in comparison to its non-redundant counterpart is given with respect to the optimization strategy. Significant improvements of the achievable accuracy are well noticeable in most cases. It can be seen that the non-redundant mechanism passes a singular configuration while moving along t_{II} with $\phi_{\mathrm{E}} = 40°$ (note: in Table II the values of the pose error [mm/°] are given instead of the percentage improvement). Thanks to the kinematic redundancy and a performed reconfiguration the singularity could be avoided.

TABLE II

MAXIMAL TRANSLATIONAL $\overline{\Delta xy}_{\mathrm{m}}$ AND ROTATIONAL ERROR $\overline{\Delta\phi_{\mathrm{E}}}_{\mathrm{m}}$ WITH RESPECT TO THE OPTIMIZATION STRATEGY WHILE MOVING ALONG TRAJECTORY t_{I} (TOP), t_{II} (CENTER), AND t_{III} (BOTTOM)

ϕ_{E}	Value	3RRR	3(P)RRR (η [%])				
		[mm/°]	1	2	3	4	5
−40°	$\overline{\Delta xy}_{\mathrm{m}}$	1.70	-47.7	-47.7	-47.7	-47.6	-47.9
	$\overline{\Delta\phi_{\mathrm{E}}}_{\mathrm{m}}$	0.52	-56.8	-56.8	-56.8	-51.0	-49.4
0°	$\overline{\Delta xy}_{\mathrm{m}}$	0.77	-4.7	-7.1	-7.1	-3.6	-6.8
	$\overline{\Delta\phi_{\mathrm{E}}}_{\mathrm{m}}$	0.36	-19.0	-30.9	-30.9	-13.9	-27.8
40°	$\overline{\Delta xy}_{\mathrm{m}}$	1.05	+7.0	+7.0	+7.0	+5.2	+6.0
	$\overline{\Delta\phi_{\mathrm{E}}}_{\mathrm{m}}$	0.56	-6.8	-6.8	-6.8	-6.5	-7.2
−40°	$\overline{\Delta xy}_{\mathrm{m}}$	∞	(0.47)	(0.47)	(0.47)	(∞)	(0.47)
	$\overline{\Delta\phi_{\mathrm{E}}}_{\mathrm{m}}$	∞	(0.12)	(0.12)	(0.12)	(∞)	(0.12)
0°	$\overline{\Delta xy}_{\mathrm{m}}$	2.24	-78.1	-77.7	-78.1	+2.5	-78.9
	$\overline{\Delta\phi_{\mathrm{E}}}_{\mathrm{m}}$	1.50	-84.4	-84.4	-84.4	+2.8	-84.3
40°	$\overline{\Delta xy}_{\mathrm{m}}$	0.87	-5.9	-5.9	-5.9	-6.3	-6.3
	$\overline{\Delta\phi_{\mathrm{E}}}_{\mathrm{m}}$	0.54	-13.4	-13.4	-13.4	-13.4	-13.4
−40°	$\overline{\Delta xy}_{\mathrm{m}}$	1.93	-15.5	-15.5	-15.5	-13.5	-13.9
	$\overline{\Delta\phi_{\mathrm{E}}}_{\mathrm{m}}$	0.63	-11.5	-11.5	-11.5	-10.2	-10.2
0°	$\overline{\Delta xy}_{\mathrm{m}}$	0.81	-3.1	-3.1	+9.4	-2.4	-2.4
	$\overline{\Delta\phi_{\mathrm{E}}}_{\mathrm{m}}$	0.41	-15.9	-19.4	-29.3	-12.8	-12.8
40°	$\overline{\Delta xy}_{\mathrm{m}}$	0.88	+19.0	+18.7	+18.7	+3.3	+15.8
	$\overline{\Delta\phi_{\mathrm{E}}}_{\mathrm{m}}$	0.53	+16.2	+11.7	+11.7	+2.4	+10.9

Sometimes, e.g. regarding t_{III} for $\phi_{\mathrm{E}} = 40°$, the pose error increases. The reason is that the optimal configuration is close to the symmetrical, i.e. the 'classical' non-redundant configuration. As a result, the additional active joint error $\Delta\delta$ leads to a decreased performance. However, this is not critical since in such cases the pose error of the non-redundant as well as of the redundant mechanism are comparatively low.

Summarizing the results given in Table II and taking the

complexity of the individual optimization strategies into account, e.g. in terms of the robot control, the authors propose an exclusively discrete-based optimization of δ. In most cases it led to appropriate δ_{opt} in terms of singularity avoidance and accuracy improvement. An (additional) continuous reconfiguration was not able to significantly outperform the comparatively simple discrete approaches. This is due to the already mentioned reason(s).

C. Further Modifications

As mentioned in Section III-A.6, DOF of the EE not being a part of the taskspace can be used to further improve the performance of a PKM. Fig. 5 shows the results when moving along t_{I}. The actuator position δ as well as the EE orientation ϕ_{E} were optimized based on the introduced discrete approach (Section III-A.2). The results give an idea

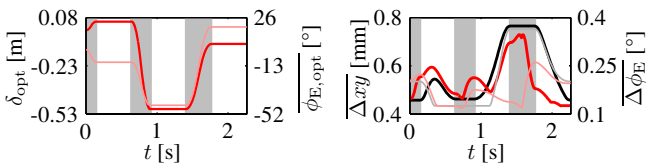

Fig. 5. Simulation results while moving along t_{I}; left: δ_{opt} (thick red) and $\phi_{\mathrm{E,opt}}$ (thin light red), right: $\overline{\Delta xy}$ (thick black: 3RRR ($\phi_{\mathrm{E}} = 0°$), thick red: 3(P)RRR) and $\overline{\Delta\phi_{\mathrm{E}}}$ (thin gray: 3RRR ($\phi_{\mathrm{E}} = 0°$), thin light red: 3(P)RRR); gray marked areas indicate a discrete reconfiguration

about the further potential when additionally using one or more redundant DOF of a mechanism's EE.

V. Conclusion

In this paper, a kinematically redundant 3(P)RRR mechanism is presented. After a description of some fundamentals, several optimization strategies for the position of the redundant actuator(s) are introduced: a single optimization, a discrete optimization, a discrete optimization in case of necessity, a continuous optimization, and a semi-continuous optimization. They are based on minimizing a criterion denoted the gain of the maximal homogenized pose error. Several analysis examples demonstrate the efficiency (in terms of an increasing performance) of kinematic redundancy with respect to the introduced optimization procedures. It is shown that an (additional) continuous reconfiguration of the mechanism is not able to significantly outperform the comparatively simple discrete optimization strategies. Concluding, the possibility of using 'unnecessary' DOF of a mechanism's EE is briefly discussed. It is demonstrated that such redundant DOF might further improve a PKM's performance.

Future work will deal with the design optimization of the prismatic actuator, e.g. its orientation with respect to the x-axis of $(\mathrm{CF})_0$ as well as its stroke ('length'). In addition, an experimental validation of the obtained numerical results will be performed.

References

[1] C. M. Gosselin and J. Angeles, "Singularity analysis of closed-loop kinematic chains," *IEEE Transactions on Robotics and Automation*, vol. 6, no. 3, pp. 281–290, June 1990.

[2] J. Kotlarski, H. Abdellatif, and B. Heimann, "Improving the pose accuracy of a planar 3RRR parallel manipulator using kinematic redundancy and optimized switching patterns," in *Proc. of the 2008 IEEE International Conference on Robotics and Automation*, Pasadena, USA, May 2008, pp. 3863–3868.

[3] J.-P. Merlet, "Redundant parallel manipulators," *Laboratory Robotics and Automation*, vol. 8, no. 1, pp. 17–24, February 1996.

[4] S. Kock and W. Schumacher, "A parallel x-y manipulator with actuation redundancy for high-speed and active-stiffness applications," in *Proc. of the 1998 IEEE International Conference on Robotics and Automation*, May 1998, pp. 2295–2300.

[5] J. Wang and C. M. Gosselin, "Kinematic analysis and design of kinematically redundant parallel mechanisms," *Journal of Mechanical Design*, vol. 126, no. 1, pp. 109–118, January 2004.

[6] S. Kock, "Parallelroboter mit Antriebsredundanz," Ph.D. dissertation, Institute of Control Engineering, TU Brunswick, Germany, March 2001.

[7] A. Müller, "Internal preload control of redundantly actuated parallel manipulators & its application to backlash avoiding control," *IEEE Transactions on Robotics and Automation*, vol. 21, no. 4, pp. 668–677, August 2005.

[8] M. G. Mohamed and C. M. Gosselin, "Design and analysis of kinematically redundant parallel manipulators with configurable platforms," *IEEE Transactions on Robotics*, vol. 21, no. 3, pp. 277–287, June 2005.

[9] S.-H. Cha, T. A. Lasky, and S. A. Velinsky, "Singularity avoidance for the 3-RRR mechanism using kinematic redundancy," in *Proc. of the 2007 IEEE International Conference on Robotics and Automation*, April 2007, pp. 1195–1200.

[10] I. Ebrahimi, J. A. Carretero, and R. Boudreau, "3-PRRR redundant planar parallel manipulator: Inverse displacement, workspace and singularity analyses," *Mechanism & Machine Theory*, vol. 42, no. 8, pp. 1007–1016, August 2007.

[11] ——, "Actuation scheme for a 6-dof kinematically redundant planar parallel manipulator," in *Proc. of the 12th IFToMM World Congress*, vol. 12, Besancon, France, June 2007.

[12] J. Kotlarski, T. Do Thanh, H. Abdellatif, and B. Heimann, "Singularity avoidance of a kinematically redundant parallel robot by a constrained optimization of the actuation forces," in *Proc. of the 17th CISM-IFToMM Symposium on Robot Design, Dynamics, and Control*, Tokyo, Japan, July 2008, pp. 435–442.

[13] V. Arakelian, S. Briot, and V. Glazunov, "Increase of singularity-free zones in the workspace of parallel manipulators using mechanisms of variable structure," *Mech Mach Theory*, vol. 43, no. 9, pp. 1129–1140, September 2008.

[14] J. Kotlarski, B. Heimann, and T. Ortmaier, *Advances in Robot Manipulators*. Vienna, Austria: I-Tech Education and Publishing, 2009, ch. Improving the Pose Accuracy of Planar Parallel Robots using Mechanisms of Variable Geometry, accepted to be published soon.

[15] C. M. Gosselin and J. Angeles, "The optimum kinematic design of a planar three-degree-of-freedom parallel manipulator," *Journal of Mechanisms, Transmissions, and Automation in Design*, vol. 110, no. 1, pp. 35–41, March 1988.

[16] J. Kotlarski, H. Abdellatif, and B. Heimann, "On singularity avoidance and workspace enlargement of planar parallel manipulators using kinematic redundancy," in *Proc. of the 13th IASTED International Conference on Robotics and Applications*, August 2007, pp. 451–456.

[17] J.-P. Merlet, "Jacobian, manipulability, condition number, and accuracy of parallel robots," *Journal of Mechanical Design*, vol. 128, no. 1, pp. 199–206, January 2006.

[18] J. Kotlarski, H. Abdellatif, T. Ortmaier, and B. Heimann, "Enlarging the useable workspace of planar parallel robots using mechanisms of variable geometry," in *Proc. of the ASME/IFToMM International Conference on Reconfigurable Mechanisms and Robots*, London, United Kingdom, June 2009, pp. 94–103.

[19] J.-P. Merlet, "Computing the worst case accuracy of a PKM over a workspace or a trajectory," in *Proc. of the 5th Chemnitz Parallel Kinematics Seminar*, April 2006, pp. 83–96.

[20] C. M. Gosselin, "Optimum design of robotic manipulators using dexterity indices," *Robotics and Autonomous Systems*, vol. 9, no. 4, pp. 213–226, 1992.

[21] R. P. Brent, *Algorithms for Minimization Without Derivatives*. New York, USA: Dover Publications, 2002.